POLYAKOV LOOP EIGENVALUES IN THE PRESENCE OF BARYON CHEMICAL POTENTIAL

O. Borisenko[1*], V. Chelnokov[1,2], S. Voloshyn[1]

[1] *Bogolyubov Institute for Theoretical Physics, National Academy of Sciences of Ukraine, 03143 Kyiv, Ukraine*

[2] *Institut für Theoretische Physik, Goethe-Universität Frankfurt, Max-von-Laue-Str. 1, 60438 Frankfurt am Main, Germany*

[*] *e-mail: oleg@bitp.kiev.ua*

The eigenvalues of the Polyakov loop are calculated in the strong coupled lattice QCD at finite temperature. This is done both in the pure gauge theory and in the theory with heavy quarks at finite baryon chemical potential. Computations are performed in the mean-field like approach to the effective action. Using the eigenvalues obtained we also evaluate the free energy, real and imaginary parts of the Polyakov loops and the baryon density. The phase diagram of the model and influence of the baryon chemical potential are discussed in details. We underline a similarity between our calculations and continuum derivations of the phenomenon of A_0 condensation.

Keywords: lattice gauge theory, deconfinement phase transition, strong coupling expansion, Polyakov loop.

Received 12.10.2020; Received in revised form 15.11.2020; Accepted 01.12.2020

1. Introduction

The deep understanding of the phase diagram of Quantum Chromodynamics (QCD) remains one of the most important problems of high energy physics (see Ref. [1] for a recent review of the problem). Among many unresolved issues, the problem of establishing a true QCD phase diagram lies at the heart of most studies conducted during the last two decades in this area of high energy physics. One of the approaches developed to attack this problem relies on the computation of the so-called A_0 condensate (in the continuum) and the eigenvalues of the Polyakov loop (on the lattice). Both quantities are related through the definition of the Polyakov loop matrix

$$U(x) \;=\; P\exp\left[i\int_0^\beta A_0(x,t)dt\right]\;,\;\;\text{(continuum)}\;, \tag{1}$$

$$U(x) \;=\; \prod_{t=1}^{N_t} U_0(x,t)\;,\;\;\text{(lattice)}\;, \tag{2}$$

where P means a path ordering and $U_0(x,t)$ is a temporal gauge matrix. An explicit relation in the static gauge will be given below. The calculation both of the condensate and the Polyakov loop has a long history. The early calculations of the condensate [2–7] and the eigenvalues [8–10] had been reviewed in [11]. The role of the invariant measure in the generation of the condensate and the eigenvalues was investigated in detail in [12]. The expectation values of the Polyakov loops and their correlations have been calculated beyond the leading order in [13]. More recent development can be found in papers [14–16]. Finally, the generation of A_0 condensate in the presence of the baryon chemical potential has been investigated in [17, 18].

In this paper we intend to study the phase structure of $SU(N)$ QCD for $N = 2, 3$ at finite temperatures and baryon densities using the effective Polyakov loop model which can be calculated in the strong coupled lattice QCD and in the region of large quark masses. We do it by evaluating the maximum of the effective Polyakov loop action and extracting thus the eigenvalues of the Polyakov loops in the points of maxima of the action. This, in turn, allows

us to compute all local observables in the theory.

The paper is organized as follows. In the next Section we describe the $SU(N)$ Polyakov loop model we deal with for all N. In Sec.3 we solve the $SU(2)$ model at finite density and outline its phase diagram. Sec.4 is devoted to a detailed study of the physically relevant $SU(3)$ model. We compute here the free energy, expectation values of the real and imaginary parts of the Polyakov loop and the baryon density. In Summary we discuss our results and compare them with analytical calculations of A_0 condensate in continuum.

2. $SU(N)$ Polyakov loop model

We shall study a model defined on a d-dimensional hypercubic lattice $\Lambda = L^d$ with periodic boundary conditions (BC) in all directions. We will denote a lattice site as $\vec{x} \equiv (x_1, ..., x_d)$, $x_i \in [0, L-1]$, and a link in direction n, $n \in [1, d]$ as $l = (\vec{x}, n)$. To each site corresponds a variable $U(x) \in G$, belonging to a gauge group G ($G = U(N), SU(N)$). $\mathrm{Tr}\, U$ is the fundamental character of G. The partition function of the model is given by

$$Z_\Lambda(\beta, m, \mu; N, N_f) \equiv Z \;=\; \int \prod_x dU(x) \prod_{x,n} B_g(\beta) \prod_x \prod_{f=1}^{N_f} B_q(m_f, \mu_f)\,, \tag{3}$$

where dU denotes the (reduced) Haar measure on G. This model is an effective model, defining interactions of Polyakov loops in a static quark limit of a $(d+1)$-dimensional lattice gauge theory with N_f flavours of quarks, each having a mass m_f and a (real) chemical potential μ_f. $B_g(\beta)$ corresponds to the gauge part of the original Boltzmann weight and $B_q(m_f, \mu_f)$ is a static quark determinant for a given flavour f with mass m_f and chemical potential μ_f.

While several choices of $B_g(\beta)$ and $B_q(m_f, \mu_f)$ were discussed in the literature, in this paper we use one of the simplest forms, obtained after explicit integration over all spatial link variables on an anisotropic lattice (see, for instance Refs. [19–21] and references therein)

$$B_g(\beta) \;=\; \exp\left[\beta_{eff}\, \mathrm{ReTr}U(x)\mathrm{Tr}U^\dagger(x+e_n)\right]\,. \tag{4}$$

The contribution of static fermions is represented in the form

$$\prod_{f=1}^{N_f} B_q(m_f, \mu_f) \;\approx\; \exp\left[\frac{h_+}{2}\mathrm{Tr}U(x) + \frac{h_-}{2}\mathrm{Tr}U^\dagger(x)\right]\,. \tag{5}$$

The parameters h_+ and h_- depend on quark masses m_f, chemical potentials μ_f, lattice size in the temporal direction N_t, and also on the choice of the lattice discretization of the fermions (Wilson or staggered fermions). The exact form of this dependance is not important in our current study. In what follows, we parametrize $h_\pm$ as $h_\pm = he^{\pm\mu}$, where $h = e^{-m}$, m is a quark mass, finally writing the partition function in the form

$$\begin{aligned} Z \;&=\; \int \prod_x dU(x) \exp\left[\beta \sum_{x,n} \mathrm{ReTr}U(x)\mathrm{Tr}U^\dagger(x+e_n)\right] \\ &\times\; \exp\left[\frac{h}{2}\sum_x \left(e^{\mu}\mathrm{Tr}U(x) + e^{-\mu}\mathrm{Tr}U^\dagger(x)\right)\right]\,. \end{aligned} \tag{6}$$

The gauge variables $U(x)$ here correspond to the Polyakov loops of the original model, as the only gauge-invariant combinations of fields remaining after the integrations. The fact that the Boltzmann weight remains invariant under local gauge transformations of variables $U(x)$ allows us to chose a gauge in which all the matrices $U(x)$ are diagonal (static diagonal gauge)

$$U(x) = \text{diag}\left(e^{i\omega_1(x)}, \cdots, e^{i\omega_N(x)}\right) \ . \tag{7}$$

In this notation $\omega_i(x)$ are defined by the linear combination $\sum_c t^c A_0^c(x)$ of the generators t_c of the group G. For example, in $SU(3)$ (a – temporal lattice spacing)

$$\frac{\omega_1}{aN_t} = A_0^3 + \frac{1}{\sqrt{3}}\, A_0^8 \ , \ \frac{\omega_2}{aN_t} = -A_0^3 + \frac{1}{\sqrt{3}}\, A_0^8 \ , \ \frac{\omega_3}{aN_t} = -\frac{2}{\sqrt{3}}\, A_0^8 \ . \tag{8}$$

In the static diagonal gauge (7) one can write explicit expressions for the elements of the partition function (6) in terms of $\omega_i(x)$

$$\begin{aligned} \mathrm{Re}\mathrm{Tr}W(x)\mathrm{Tr}W^\dagger(x+e_n) \ &= \ \sum_{i,j=1}^{N} \cos\left[\omega_i(x) - \omega_j(x+e_n)\right] \ , \\ e^{\mu}\mathrm{Tr}U(x) + e^{-\mu}\mathrm{Tr}U^\dagger(x) \ &= \ 2\sum_{i=1}^{N} \cos\left[\omega_i(x) - i\mu\right] \ , \\ \int dU \ = \ \int_0^{2\pi} D(\omega)D^\star(\omega)\ \delta(\omega) \prod_{k=1}^{N} \frac{d\omega_k}{2\pi} \ , \quad D(\omega) \ &= \ \prod_{k<l} \left(e^{i\omega_k} - e^{i\omega_l}\right) \ , \end{aligned} \tag{9}$$

where the $SU(N)$ constraint on the matrix eigenvalues is implemented by a periodic delta function

$$\delta(\omega) \ = \ \sum_{q=-\infty}^{\infty} \exp\left[iq\sum_{k=1}^{N}\omega_k\right] \ . \tag{10}$$

This constraint reduces global symmetry transformations of the pure gauge model from continuous $U(1)$ symmetry to a discrete $Z(N)$ symmetry $\omega_k(x) \to \omega_k(x) + \frac{2\pi n}{N}$. The introduction of the quark contribution explicitly violates the global $Z(N)$ symmetry, and, for nonzero μ, makes the Boltzmann weight complex, preventing the direct Monte Carlo simulation of the model.

The model defined in Eq.(6) was extensively studied. In [22] it was shown that in the $U(3)$ model the dependence on the chemical potential vanishes, thus making the Boltzman weight for the whole configuration real. This result is easily generalized to arbitrary $U(N)$ model. In [23] a large-N limit of the $U(N)$ model has been investigated. It was shown that the model undergoes a third-order phase transition. An extension of this result to the large-N limit of the $SU(N)$ model was done in [24]. The $SU(3)$ model was studied using the mean-field approach in [22, 25]. The dual formulations free of sign problem were proposed in [26–28], and used for Monte-Carlo simulations of the model in [20, 29, 30]. These studies reveal (at least in some parameter regions) the phase diagram of the model.

At large β and/or $h_\pm$ the model (6) can be approximately solved by first finding the saddle-points for group integrals and then by evaluating the integrals over fluctuations around the saddles. We are interested in constructing a constant, translationally-invariant solution which provides global maximum of the action. Using Eqs.(9)-(10) it is strightforward to get the following

system of saddle-point equations for $U(N)$

$$\sum_{j;j\neq k}\left(\gamma\cot\frac{1}{2}(\omega_k-\omega_j)-2d\beta\sin(\omega_k-\omega_j)\right) \;=\; h\sin(\omega_k-i\mu)\;. \tag{11}$$

The constant γ has been introduced here in front of contribution from the invariant measure. One should put $\gamma=1$ after calculations. For $SU(N)$ case the system of equations remain the same but it must be supplemented by additional equation which takes into account the constraint on the determinant of $SU(N)$ matrices (10)

$$\sum_{i=1}^{N}\omega_i \;=\; 2\pi q\;. \tag{12}$$

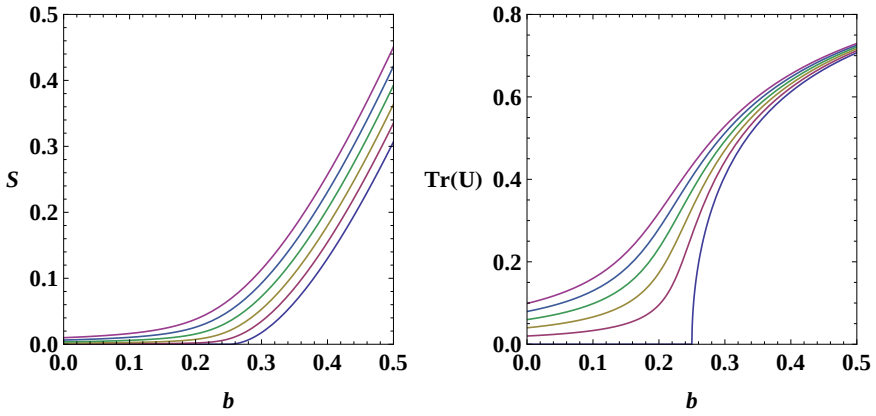

Fig. 1. Plots of the free energy (13) (left) and the Polyakov loop trace(17) (right), for $\mu=0$ as functions of $d\beta$. Different lines (distinguished by color) correspond from bottom to top to $h=0.0,0.02,0.04,0.06,0.08,0.1$

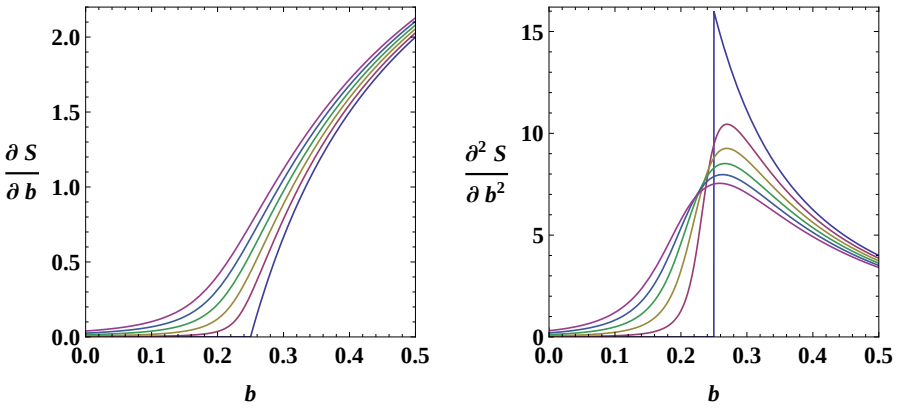

Fig. 2. Plots of the first (left) and second (right) derivatives of the free energy for $\mu=0$ as functions of $d\beta$. Different lines (distinguished by color) correspond from bottom to top to $h=0.0,0.02,0.04,0.06,0.08,0.1$

3. Phase diagram of $SU(2)$ model

As a simple example consider $SU(2)$ model. At finite chemical potential the classical action of $SU(2)$ remains real and depends on μ only as $v = h\cosh\mu$

$$S_{cl} \;=\; 2b(1+\cos 2\omega) + 2v\cos\omega + 2\log\sin\omega\;. \tag{13}$$

Here, $b = d\beta$. In terms of variable $t = \cos\omega$ the action (13) leads to a cubic equation which has three solutions. The relevant one reads

$$t(b,v) \;=\; \frac{1}{12b}\left[-v + \frac{p_1}{\sqrt[3]{p_2+\sqrt{p_2^2-p_1^3}}} + \sqrt[3]{p_2+\sqrt{p_2^2-p_1^3}}\right], \tag{14}$$

$$p_1 \;=\; 12b(4b-1)+v^2;\;\; p_2 \;=\; 18b(1+8b)v - v^3\;. \tag{15}$$

In the pure gauge case it reduces to

$$t(b,0) \;=\; \begin{cases} 0,\; b \le \frac{1}{4}\;; \\ \sqrt{1-1/4b},\; b \ge \frac{1}{4}\;. \end{cases} \tag{16}$$

Only in the pure gauge case we have a genuine phase transition which turns out to be of the second order, as can be seen from the plots of the free energy in the left panel of Fig. 1, and its first and second derivative as a function of $b = d\beta$ shown in Fig. 2: while the first derivative is continuous, the second one exhibits a finite jump. At any non-zero h all derivatives are continuous functions of b.

The Polyakov loop becomes

$$\mathrm{Tr}U = \cos\omega = t(b,v)\;. \tag{17}$$

We would like to note that $SU(2)$ Polyakov loop remains real even at non-zero μ. The plots of the real part of the $SU(2)$ Polyakov loop as a function of $b = d\beta$ are shown in Fig. 1, right panel.

Finally, we have also computed the baryon density as a derivative of the free energy with respect to chemical potential. Its behaviour is shown in Fig. 3. As expected, the density is a growing function of the chemical potential.

4. Phase diagram of $SU(3)$ model

A more sophisticated example is the $SU(3)$ model. This case suffers from a sign problem. In this case Eqs.(11) and (12) lead to the system of two equations. With the substitution

$$x \;=\; \frac{3}{2}(\omega_1+\omega_2)\;,\; 0 \le x \le 6\pi\;,\; y \;=\; \frac{1}{2}(\omega_1-\omega_2)\;,\; -\pi \le y \le \pi\;. \tag{18}$$

the classical action for $N = 3$ and $\gamma = 1$ takes a form

$$\begin{aligned} S_{cl} \;&=\; 3b + 2b\left[\cos 2y + \cos(x+y) + \cos(x-y)\right] + 2\ln\left[\sin y \sin\frac{x+y}{2}\sin\frac{x-y}{2}\right] \\ &+\; h\cos\left(\frac{x}{3}+y-i\mu\right) + h\cos\left(\frac{x}{3}-y-i\mu\right) + h\cos\left(\frac{2x}{3}+i\mu\right)\;. \end{aligned} \tag{19}$$

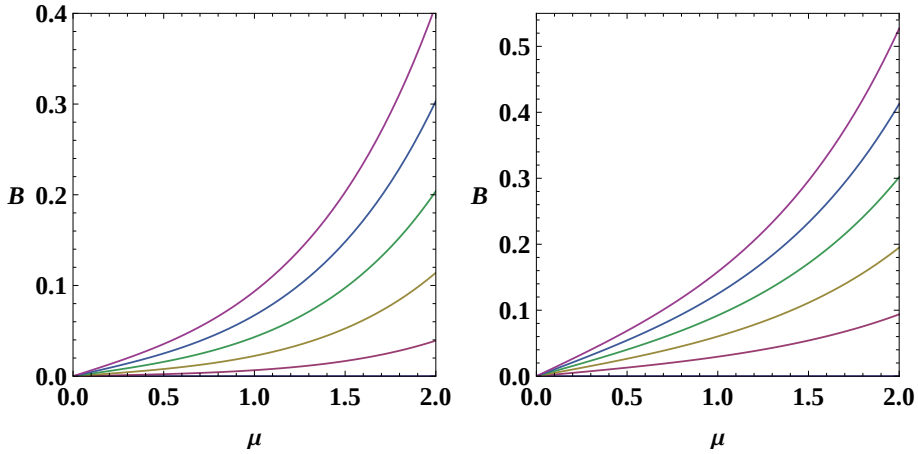

Fig. 3. Plots of the baryon density at $\beta d = 0.2$ (left) and $\beta d = 0.4$ (right) as a function of μ. Different lines (distinguished by color) correspond from bottom to top to $h = 0.0, 0.02, 0.04, 0.06, 0.08, 0.1$.

After some algebra one gets the following system of equations

$$\begin{aligned}
&\sin x\,[2b\cos y(\cos x-\cos y)+1]\\
&+\frac{h}{3}\,(\cos x-\cos y)\,\left[\sin\left(\frac{x}{3}-i\mu\right)\cos y+\frac{1}{2}\sin\left(\frac{2x}{3}+i\mu\right)\right]\;=\;0\,, \qquad (20)\\
&2b\sin^2 y\,(\cos x-\cos y)\,(\cos x+2\cos y)-\left(1+\cos x\cos y-2\cos^2 y\right)\\
&+h\sin^2 y\,(\cos x-\cos y)\,\cos\left(\frac{x}{3}-i\mu\right)\;=\;0\,. \qquad (21)
\end{aligned}$$

The Polyakov loop becomes

$$\begin{aligned}
\mathrm{Tr}U\;&=\;\cos\omega_1+\cos\omega_2+\cos(\omega_1+\omega_2)+i\sin\omega_1+i\sin\omega_2-i\sin(\omega_1+\omega_2)\\
&=\;2\cos\frac{x}{3}\cos y+\cos\frac{2x}{3}+2i\sin\frac{x}{3}\cos y-i\sin\frac{2x}{3}\,. \qquad (22)
\end{aligned}$$

Comparing with formula (8) one concludes that $y \sim A_0^3$ and $x \sim A_0^8$.

4.1. Pure gauge theory

Consider first the pure gauge theory, i.e. $h = 0$. The system of Eqs.(20)-(21) simplifies to

$$\begin{aligned}
\sin x\,[2b\cos y(\cos x-\cos y)+1]\;&=\;0\,, \qquad (23)\\
2b\sin^2 y\,(\cos x-\cos y)\,(\cos x+2\cos y)-\left(1+\cos x\cos y-2\cos^2 y\right)\;&=\;0 \qquad (24)
\end{aligned}$$

and has the following solutions:

I. Confinement phase:

$$\begin{aligned}
A:\quad & x_c\;=\;2k\pi\,,\;y_c\;=\;\pm\frac{2\pi}{3}\,,\;k=0,1,2\,;\\
B:\quad & x_c\;=\;(2k+1)\pi\,,\;y_c\;=\;\pm\frac{\pi}{3}\,,\;k=0,1,2\,. \qquad (25)
\end{aligned}$$

These solutions describe the confinement phase. One finds the real and imaginary parts of the

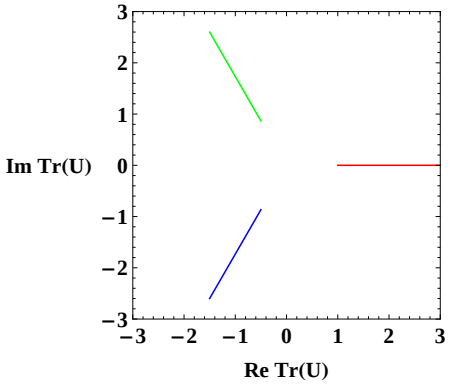

Fig. 4. Parametric plots of the Polyakov loops (30) above critical point in three $Z(3)$ degenerate phases.

Polyakov loop and the classical action which are the same on all solutions

$$\text{Re Tr}U(x_c, y_c) \;=\; \text{Im Tr}U(x_c, y_c) \;=\; 0\,, \tag{26}$$

$$S_{conf}(x_c, y_c) \;=\; -3\ln\frac{4}{3}\,. \tag{27}$$

II. Deconfinement phase:

$$x_d \;=\; k\pi\,,\; \sin y_d \;=\; \frac{1}{\sqrt{2b}}\,,\; \cos y_d \;=\; z_d \;=\; \sqrt{1-1/2b}\,;\; k = 0,1,2,3,4,5\,. \tag{28}$$

These solutions describe the deconfinement phase. The value $x_d = 0$ corresponds to $A_0^8 = 0$. The action (19) with $k = 0, 2, 4$ is degenerate on these solutions and equals

$$S_{dec}(x_d = 0, 2\pi, 4\pi, y_d) \;=\; -2 - 5\ln 2 - 3\ln b + 5b + 4z_d - 2\ln(1+z_d)\;. \tag{29}$$

The corresponding values of the Polyakov loop

$$\begin{aligned}
&\text{Re Tr}U(x_d = 0) = 1 + 2z_d\,,\; \text{Im Tr}U(x_d = 0) = 0\,, \\
&\text{Re Tr}U(x_d = 2\pi) = -\frac{1}{2} - z_d\,,\; \text{Im Tr}U(x_d = 2\pi) = \sqrt{3}\left(\frac{1}{2} + z_d\right), \\
&\text{Re Tr}U(x_d = 4\pi) = -\frac{1}{2} - z_d\,,\; \text{Im Tr}U(x_d = 4\pi) = -\sqrt{3}\left(\frac{1}{2} + z_d\right)
\end{aligned} \tag{30}$$

describe the $Z(3)$ degenerate phases of $SU(3)$ gauge theory above the deconfinement phase transition. Solutions with $x_d = 0, 2\pi, 4\pi$ provide the global maximum of the action (19). Their appearance signals the spontaneous symmetry breaking of the global $Z(3)$ symmetry above the critical point. The critical point is found from the equation $S_{conf} = S_{dec}$ and equals $\beta_c \approx 1/6$. This is a first order phase transition because the order parameter – the Polyakov loop, as well as the first derivative of the free energy, exhibits a jump across the critical point. The parametric plots of the real and imaginary parts of the Polyakov loop as a function of $b = d\beta$ are shown in Fig. 4. The odd values of $k = 1, 3, 5$ correspond to minima of the classical action.

4.2. Theory with static quarks

When $h > 0$ the degeneracy of the solution of the equations (20)-(21) is removed. This is a consequence of a breaking of the global $Z(3)$ symmetry when dynamical quarks are added to

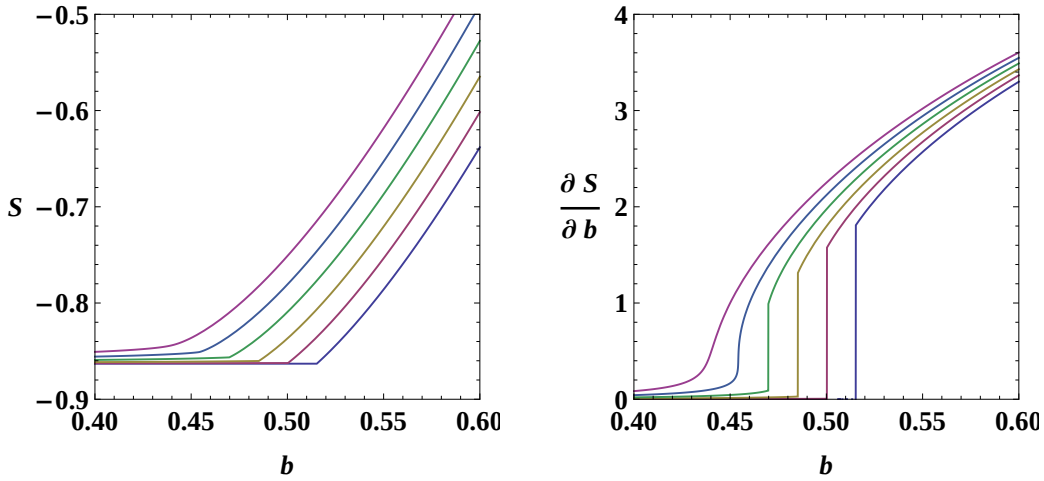

Fig. 5. $SU(3)$ **model free energy (19) (left) and its derivative (right) for** $\mu = 0$ **as functions of** $d\beta$**. Different lines (distinguished by color) belongs from down to top to** $h = 0.0, 0.02, 0.04, 0.06, 0.08, 0.1$**.**

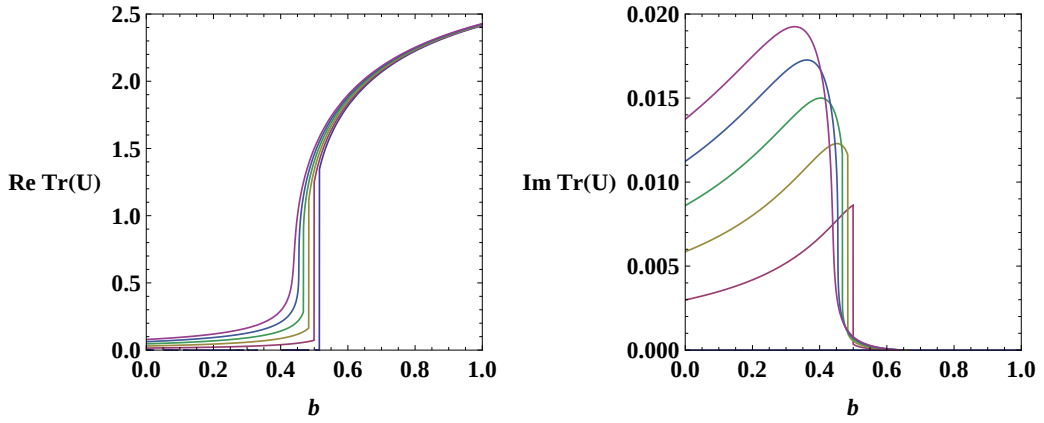

Fig. 6. The real (left) and imaginary (right) parts of the Polyakov loops (22) for $\mu = 0.3$ **as a function of** $b = d\beta$**. Different lines (distinguished by color) correspond from bottom to top to** $h = 0.0, 0.02, 0.04, 0.06, 0.08, 0.1$**.**

the action.

Unlike the $SU(2)$ case, the system of equations for the $SU(3)$ model cannot be solved exactly when both h and μ are non-zero. First, from the analysis of the equations (20, 21) one can see that the solution for x in presence of a real chemical potential should be imaginary. In what follows we do a change of variables $x \to i\,x$, which causes the imaginary part of the Polyakov loop to be purely imaginary.

We search for the solution in the form of a series expansion in powers of u (where $v = h\cosh\mu$, $u = \tanh\mu$)

$$x \;=\; u x_1(b,v) + O\left(u^3\right)\;, \tag{31}$$

$$t = \cos y \;=\; t_0(b,v) + u^2 t_2(b,v) + O\left(u^4\right)\;. \tag{32}$$

From symmetries of equations one observes that x includes only odd powers and t includes only even powers of u.

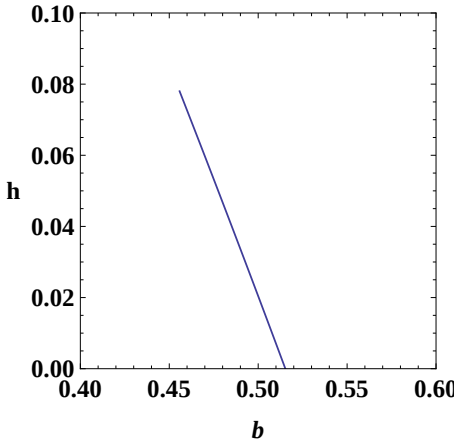

Fig. 7. Phase transition line in the plane b-h at $\mu = 0$.

We find for x, t

$$x_1 = \frac{v(t_0-1)(2t_0-1)}{2(v(t_0^2-1)+18b(t_0-1)t_0-9}\ , \tag{33}$$

$$t_2 = x_1\frac{(t_0^2-1)[18b\,x_1(2+t_0)-v(2+t_0(x_1-2))-10x_1]+9t_0x_1}{4b(t_0-1)(t_0(5+8t_0)-1)-2(1+v)+2t_0(4+v(3t_0-2))}\ , \tag{34}$$

where t_0 is a root of a cubic equation

$$t_0^1(b,v) \;=\; \frac{1}{12b}\left[-(2b+v)+\frac{d_1}{\sqrt[3]{d_2+\sqrt{d_2^2-d_1^3}}}+\sqrt[3]{d_2+\sqrt{d_2^2-d_1^3}}\right], \tag{35}$$

$$t_0^{2,3}(b,v) = -\frac{1}{12b}\left[(2b+v)+\frac{(1\pm i\sqrt{3})\,d_1}{2\sqrt[3]{d_2+\sqrt{d_2^2-d_1^3}}}+\frac{1\mp i\sqrt{3}}{2}\sqrt[3]{d_2+\sqrt{d_2^2-d_1^3}}\right], \tag{36}$$

$$d_1 \;=\; 52b^2+4b(v-6)+v^2\ ,\ \ d_2 \;=\; 280b^3-6b(v-6)v+12b^2(11v-12)-v^3\ . \tag{37}$$

For $h < 0.07875$ all three solutions are relevant, while for $h > 0.07875$ only the first one is important. The value $h = 0.07875$ corresponds to a second order phase transition endpoint at $\mu = 0$. The limit $h \to 0$ reduces to the pure gauge case (28) (that is also a multivalued function):

$$t_0(b,0) \;=\; \begin{cases} -\frac{1}{2},\ b \le \frac{2}{3}\ ; \\ -\sqrt{1-1/2b},\ \frac{1}{2} \le b \le \frac{2}{3}\ ; \\ \sqrt{1-1/2b},\ b \ge \frac{1}{2}\ . \end{cases} \tag{38}$$

The phase transition from the confinement to the deconfinement phase is characterized by a jump of both real and imaginary parts of average Polyakov loop (at $\mu = 0$ the imaginary part is exactly zero). This is typical for the phase transitions of first order. The plots of the real and imaginary parts of the Polyakov loop as a function of $b = d\beta$ are shown in Fig. 6. On the Fig. 7 we show a cross-section of the phase transition surface by a plane $\mu = 0$.

Baryon potential as a function of μ exhibits a rapid growth. On the Fig. 8 we show a series of plots of the baryon density as a function of μ at different values of h in the confinement and

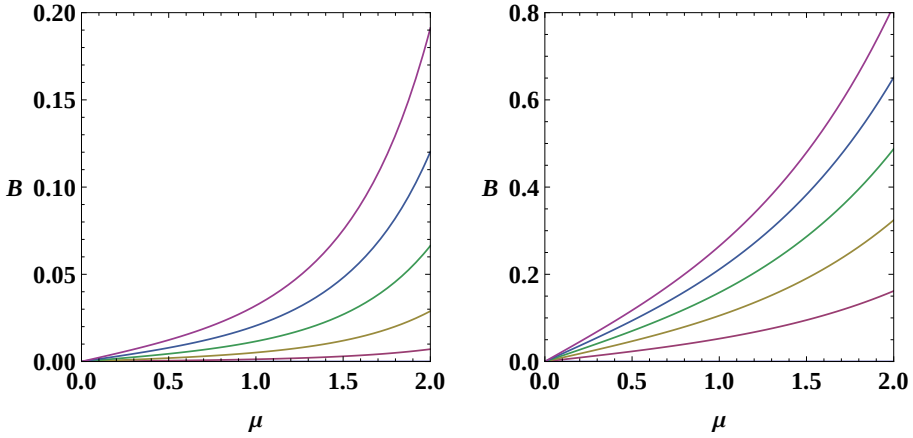

Fig. 8. Baryon density as a function of μ at the $b = 0.3$ (left) and at the $b = 0.8$ (right). Different lines (distinguished by color) correspond from down to top to $h = 0.0, 0.02, 0.04, 0.06, 0.08, 0.1$.

the deconfinement phases. Similar to the $SU(2)$ case, the baryon density is a growing function of the chemical potential.

At all fixed μ we have a critical point in h, above which the first order phase transition disappears. This points, that for the small values of μ are approximated by a curve $h\cosh(\mu) \approx 0.07875$ form a second order critical line. Above this line one observes a rapid crossover.

5. Summary

In this paper we have studied the phase structure of $SU(N)$ Polyakov loop models for $N = 2, 3$. These models can be derived from the lattice QCD in the region of the strong coupling and the large quark mass. The idea was to determine the eigenvalues of the Polyakov loop from the positions of maxima of the effective action. We did it both for the pure gauge theory and for the theory with heavy quarks in the presence of the baryon chemical potential. This allowed us to reveal the phase diagram of the models and describe the corresponding phase transitions. In addition, we have also computed the free energy and its first and second derivatives with respect to the effective coupling, as well as the baryon density. The knowledge of the eigenvalues led to a direct determination of the expectation values of the real and imaginary parts of the Polyakov loop.

At finite density two independent eigenvalues of the Polyakov loop in $SU(3)$ model become non-trivial leading to a non-vanishing value of the imaginary part of the Polyakov loop. This agrees well with the result of Ref. [18] where it was shown that when $\mu \neq 0$ the component A_0^8 acquires a non-zero imaginary value.

The further development can include investigation of the screening masses at finite density. Such masses should be extracted from the Polyakov loop correlation which, in turn can be evaluated by an integration over fluctuations around established eigenvalues. These calculations are now in progress.

Acknowledgements

V.C. acknowledges support by the Deutsche Forschungsgemeinschaft (DFG, German Research Foundation) through the CRC-TR 211 'Strong-interaction matter under extreme conditions' – project number 315477589 – TRR 211.

References

1. **Philipsen, O.** Constraining the phase diagram of QCD at finite temperature and density [Text] / O. Philipsen // PoS. – 2019. – LATTICE2019 : 273.
2. **Anishetty, R.** Chemical Potential for $SU(N)$ Infrared Problem [Text] / R. Anishetty // J. Phys. – 1984. – G 10 : 423.
3. **Enqvist, K.** Hot Gluon Matter in a Constant A_0 Background [Text] / K. Enqvist, K. Kajantie // Z. Phys. – 1990. – C 47 : 291–296.
4. **Belyaev, V.M.** Order parameter and effective potential [Text] / V. M. Belyaev // Phys. Lett. – 1991. – B 254 : 153–157.
5. **Sawayanagi, H.** Gauge fields and gauge symmetry at high temperature: Possibility of a vacuum expectation value of $O(g^2T)$ [Text] / H. Sawayanagi // Phys. Rev. – 1992. – D 45 : 3823–3832.
6. **Skalozub, V.V.** Gauge invariance of the gluon field condensation phenomenon in finite temperature QCD [Text] / V. V. Skalozub // Int. J. Mod. Phys. – 1994. – A 9 : 4747–4758.
7. **Skalozub, V.V.** Two loop contribution of quarks to the condensate of the gluon field at finite temperatures [Text] / V. V. Skalozub, I. V. Chub // Phys. Atom. Nucl. – 1994. – 57 : 324–330.
8. **Borisenko, O.** A_0 condensate in high-temperature phase of lattice QCD [Text] / O. Borisenko, V. Petrov, G. Zinovjev // Phys. Lett. – 1991. – B 264 : 166–172.
9. **Boháčik, J.** Supplementing analysis of deconfined phase in lattice QCD thermodynamics [Text] / J. Boháčik, O. Borisenko, V. Petrov, G. Zinovjev // Mod. Phys. Lett. – 1991. – A 6 : 1429–1435.
10. **Boháčik, J.** Analysis of the deconfinement phase in lattice QCD thermodynamics [Text] / J. Boháčik, O. Borisenko, V. Petrov, G. Zinovjev // Sov. J. Nucl. Phys. – 1991. – 54 : 491-493.
11. **Borisenko, O.** A_0 Condensate in QCD [Text] / O. A. Borisenko, J. Boháčik, V. V. Skalozub // Fortsch. Phys. – 1995. – 43 : 301–348.
12. **Borisenko, O.** Invariant measure in hot gauge theories [Text] / O. Borisenko, J. Boháčik // Phys. Rev. – 1997. – D 56 : 5086–5096.
13. **Brambilla, N.** The Polyakov loop and correlator of Polyakov loops at next-to-next-to-leading order [Text] / N. Brambilla, J. Ghiglieri, P. Petreczky, A. Vairo // Phys. Rev. – 2010. – D 82 : 074019.
14. **Dumitru, A.** Two-loop perturbative corrections to the thermal effective potential in gluodynamics [Text] / A. Dumitru, Y. Guo, C. P. Korthals Altes // Phys. Rev. – 2014. – D 89 : 016009.
15. **Korthals Altes, C.P.** Potential for the phase of the Wilson line at nonzero quark density [Text] / C. P. Korthals Altes, R. D. Pisarski, A. Sinkovics // Phys. Rev. – 2000. – D 61 : 056007.
16. **Korthals Altes, C.P.** Free energy of a holonomous plasma [Text] / C. P. Korthals Altes, H. Nishimura, R. D. Pisarski, V. Skokov // Phys. Rev. – 2020. – D 101 : 094025.
17. **Guo, Y.** Two-loop perturbative corrections to the constrained effective potential in thermal QCD [Text] / Y. Guo, Q. Du // JHEP – 2019. – 05 : 042.
18. **Bordag, M.** A_0–condensation in quark-gluon plasma with finite baryon density [Text] / M. Bordag, V. Skalozub // e-print arXiv:2009.11734 [hep-th].
19. **Billo, M.** Finite Temperature Lattice QCD in the Large N Limit [Text] / M. Billo, M. Caselle, A. D'Adda, S. Panzeri // Int. J. Mod. Phys. – 1997. – A 12 : 1783–1845.

20. **Fromm, M.** The QCD deconfinement transition for heavy quarks and all baryon chemical potentials [Text] / M. Fromm, J. Langelage, S. Lottini, O. Philipsen // JHEP – 2012. – 01 : 042.
21. **Langelage, J.** Heavy dense QCD and nuclear matter from an effective lattice theory [Text] / J. Langelage, M. Neuman, O. Philipsen // JHEP – 2014. – 09 : 131.
22. **Greensite, J.** Mean field theory of effective spin models as a baryon fugacity expansion [Text] / J. Greensite, K. Splittorff // Phys. Rev. – 2012. – D 86 : 074501.
23. **Christensen, C.H.** Exact Large-N_c Solution of an Effective Theory for Polyakov Loops at Finite Chemical Potential [Text] / C. H. Christensen // Phys. Lett. – 2012. – B 714 : 306–308.
24. **Borisenko, O.** The large N limit of $SU(N)$ integrals in lattice models [Text] / O. Borisenko, V. Chelnokov, S. Voloshyn // Nucl. Phys. – 2020. – B 960 : 115177.
25. **Greensite, J.** Comparison of complex Langevin and mean field methods applied to effective Polyakov line models [Text] / J. Greensite // Phys. Rev. – 2014. – D 90 : 114507.
26. **Gattringer, C.** Flux representation of an effective Polyakov loop model for QCD thermodynamics [Text] / C. Gattringer // Nucl. Phys. – 2011. – B 850 : 242–252.
27. **Borisenko, O.** Duals of $U(N)$ LGT with staggered fermions [Text] / O. Borisenko, V. Chelnokov, S. Voloshyn // Eur. Phys. J. Web of Conferences. – 2018. – 175 : 11021.
28. **Borisenko, O.** Dual formulations of Polyakov loop lattice models [Text] / O. Borisenko, V. Chelnokov, S. Voloshyn // Phys. Rev. – 2020. – D 102 : 014502.
29. **Mercado, Y.D.** Monte Carlo simulation of the $SU(3)$ spin model with chemical potential in a flux representation [Text] / Y. D. Mercado, C. Gattringer // Nucl. Phys. – 2012. – B 862 : 737–750.
30. **Borisenko, O.** Dual simulation of a Polyakov loop model at finite baryon density: phase diagram and local observables [Text] / O. Borisenko, V. Chelnokov, E. Mendicelli, A. Papa // e-print arXiv:2011.08285 [hep-lat].